

Transient and stationary behavior of the Olami-Feder-Christensen earthquake model

Felix Wissel and Barbara Drossel

Institut für Festkörperphysik, TU Darmstadt, Hochschulstraße 6, 64289 Darmstadt, Germany

(Dated: July 10, 2018)

Using long-term computer simulations and mean-field like arguments, we investigate the transient time and the properties of the stationary state of the Olami-Feder-Christensen earthquake model as function of the coupling parameter α and the system size N . The most important findings are that the transient time diverges nonanalytically when α approaches zero, and that the avalanche-size distribution will not approach a power law with increasing system size.

PACS numbers: 05.65.+b, 45.70.Ht

I. INTRODUCTION

The Olami-Feder-Christensen (OFC) earthquake model [1] is probably the most studied nonconservative and supposedly self-organized critical (SOC) model. Systems are called self-organized critical if they reach a stationary state characterized by power laws without the need for fine-tuning an external parameter such as the temperature. Many researchers in the field agree on confining the term self-organized critical to those systems that are slowly driven and that display fast, avalanche-like dissipation events. This means that there is a separation of time scales, which can be interpreted as a way of tuning a parameter to a small value [2].

The prominent example for self-organized criticality is the sand-pile model by Bak, Tang and Wiesenfeld [3] (BTW), where it can be shown analytically that the avalanche-size distribution is a power law, implying a scale invariance: Avalanches of all sizes are due to the same mechanism. The BTW model satisfies a local conservation law, which can naturally lead to power laws [4, 5], and without local particle conservation the model is not critical [2]. The mechanisms leading to SOC in nonconservative systems are not yet well understood, and for the OFC model there is yet no agreement on whether it is critical at all. While some authors find critical behavior when going to larger systems sizes and employing multiscaling methods [6, 7], others interpret similar data as showing a breakdown of scaling [8], and groups using branching-ratio techniques claim to find what they call *almost criticality* [9, 10].

Despite the simplicity of its dynamical rules, the OFC model shows a variety of interesting features that are unknown in equilibrium physics and appear to be crucial for generating the apparent critical (or almost critical) behavior. Among these features are a marginal synchronization of neighboring sites driven by the open boundary conditions [11], and the violation of finite-size scaling [7, 12] together with a qualitative difference between system-wide earthquakes and smaller earthquakes [6]. Also, small changes in the model rules (such as replacing open boundary conditions with periodic boundary conditions [13], introducing frozen noise in the local degree of dissipation [14] or in the threshold values [15], including

lattice defects [16]), destroy the SOC behavior. Recently, it was found that the results of computer simulations are strongly affected by the computing precision [17], and that the model exhibits sequences of foreshocks and aftershocks [18, 19]. If energy input occurs in discrete steps instead of continually and if thresholds are random but not quenched, one finds quasiperiodicity combined with power laws [20]. The SOC behavior fully breaks down in OFC systems in one dimension [21], where only small and system-wide avalanches are observed.

Since dynamics become extremely slow for large system sizes and for small values of the control parameter (implying strong dissipation) it is very difficult to obtain reliable results for the model based on computer simulations only. Thus, we find in the literature contradicting results concerning the transient time needed for the invasion of the ‘self-organized region’ from the boundary into the middle of the system, and concerning the avalanche-size distribution. While the transient time is found by some authors to scale with system size with an exponent depending on the level of dissipation [11], this exponent is found by others to be a constant [22], while still others find that above some critical degree of dissipation the invasion stops and never proceeds to the system’s center [12].

Similarly, the avalanche-size distribution is found either to be a power law with an universal exponent independent of the level of dissipation for large enough system sizes (however, different values for this exponent are reported in [23] and in [6, 7]), or a power law with a nonuniversal exponent [11, 24]. Some authors found no power law at all above a critical degree of dissipation, but disagree on the value above which no power laws occur [25, 26]. Still other authors suggest that the dissipative OFC model is not critical at all (just like the random-neighbor version of the model [27], which is a mean field approximation [28, 29, 30]), but displays the new feature of being close to criticality, as mentioned above. If this is correct, only the conservative case leads to power laws in the distribution of avalanches [8, 9].

By combining extensive computer simulations with analytical arguments, we will in this paper propose a phenomenological theory for the transient as well as the stationary behavior particularly in the limit of large dissipation. The most important conclusions are that the

transient time diverges nonanalytically when the control parameter α approaches zero, and that the avalanche-size distribution will not approach a power law with increasing system size.

The outline of the rest of this paper is as follows: In the next section, we present the definition of the model and explain the simulation algorithm. Then, we investigate the transient dynamics that brings the system from a random initial state to the stationary state as function of the system size and the model parameter. Section IV investigates the scaling behavior of the self-organized patches displayed by the system in the stationary state. The results flow into the interpretation of our simulation results for the avalanche-size distribution, which is studied in Section V. Finally, in Section VI, we summarize and discuss our findings.

II. THE MODEL

The OFC model originated by a simplification of the spring-block model by Burridge and Knopoff [31]. To each site of a square lattice we assign a continuous variable $z_{ij} \in [0, 1]$ that represents the local energy. Starting with a random initial configuration taken from a constant distribution, the value z of all sites is increased at a uniform rate until a site ij reaches the threshold value $z_t = 1$. This site is then said to topple, which means that the site is reset to zero and an energy $\alpha \times z_{ij}$ is passed to every nearest neighbor. If this causes a neighbor to exceed the threshold, the neighbor topples also, and the avalanche continues until all $z_{kl} < 1$. Then the uniform increase resumes. The number of topplings defines the size s of an avalanche or ‘earthquake’. The coupling parameter α can take on values in $(0, 0.25)$. Smaller α means more dissipation, and $\alpha = 0.25$ corresponds to the conservative case. Apart from the system size N , the edge length of the square lattice, α is the only parameter of the model. Except for the initial condition, the model is deterministic. After a transient time, the system reaches an attractor of its dynamics. For periodic boundary conditions, the attractor is marginally stable and has a period of N^2 topplings for all α [12, 17]. All avalanches have the size 1, and a site topples again only after all its nearest neighbors have toppled. Measured in units of energy input per site, the period is $1 - 4\alpha$. The behavior of the model is completely different for open boundary conditions, where sites at the boundary receive energy only from 3 or 2 neighbors and topple therefore on an average less often than sites in the interior. This leads to the formation of ‘patches’ of sites with a similar energy, and this patch formation proceeds from the boundaries inwards. We are using open boundary conditions throughout this paper.

Computer simulations of the model suffer from the long times needed to reach the stationary state for large N or small α . Most of the time is spent on searching for the site that will start the next avalanche, i.e. for the site

with the largest value of z . Grassberger therefore used an algorithm that searches only among the sites with the largest values of z [12]. In our simulations, we used a different algorithm, based on a hierarchical search. The system size is chosen to be a power of 2. The system is divided into 4 boxes, each of which is again divided into 4 boxes, etc., down to the box on the lowest level, which consists of 4 lattice sites. Each box knows which of its 4 subboxes contains the site with the largest z value. Thus, the number of steps to find the site with the largest z value is $\log_2 N$, since after an avalanche only those boxes have to be updated that have been affected by the avalanche.

III. TRANSIENT TIME

The transient time is the time needed for the patch formation to reach the center of the system. Figure 1 shows a system with $N = 128$ and $\alpha = 0.09$ at three different times, the last snapshot being taken in the stationary state.

One clearly distinguishes the patches close to the boundaries and the disordered inner part of the system, which behaves as if it was part of a periodic system. The time needed to establish a patchy boundary starting from a random initial configuration is very short, and virtually all of the transient time is needed to expand the patchy region to the entire system. The patches become larger with increasing distance from the boundary.

The first ones to investigate the transient behavior were Middleton and Tang [11], who found that the transient time increases as a power of N , with an exponent that depends on α . Later work on larger systems and for values of α larger than 0.15 by Lise [22] found an exponent around 1.3, which does not depend on α .

We will argue that the exponent does indeed depend on α , and that it diverges for $\alpha \rightarrow 0$. Figure 2 shows our simulation results for the transient time for different system sizes N as function of α .

Each data point is based on the simulation of one system. Averaging over several initial conditions is not possible because of the long computation times. The transient time increases with increasing α and L , and it appears to diverge for $\alpha \rightarrow 0$. For small α , one might therefore obtain the impression that the dynamics get completely stuck before the disordered block vanishes, as was suggested by Grassberger [12]. However, we found no solid evidence and no good reason why this process should stop before the patches fill the entire system. The dash-dotted lines in Figure 2 are a fit with the Ansatz (14), which is a generalized version of the result obtained in the following by using mean-field like arguments.

We start with a local balance equation, which will lead us to an expression for the toppling profile as function of time. This consideration is similar to the one applied in [21] to the one-dimensional model. Let t_{ij} be the mean number of topplings of site ij per unit time. If site ij top-

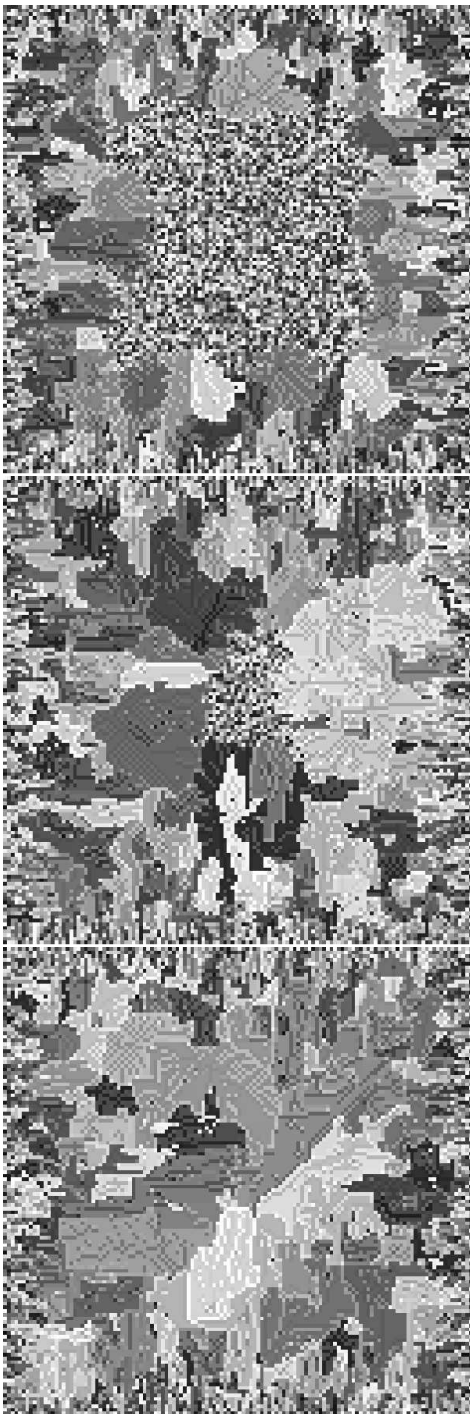


FIG. 1: Snapshots for a system with $N = 128$, $\alpha = 0.09$ after 10^5 , 5×10^5 and 8×10^5 topplings per site

ples usually when z_{ij} is at the threshold (and not above), t_{ij} must equal the mean amount of energy that this site obtains per unit time. For small values of α this assumption is well satisfied. Let g denote the rate of uniform energy input, and let $\tilde{\alpha}$ denote the average amount of energy passed to a neighbor during a toppling event. For small α , the value of $\tilde{\alpha}$ deviates very little from α , and

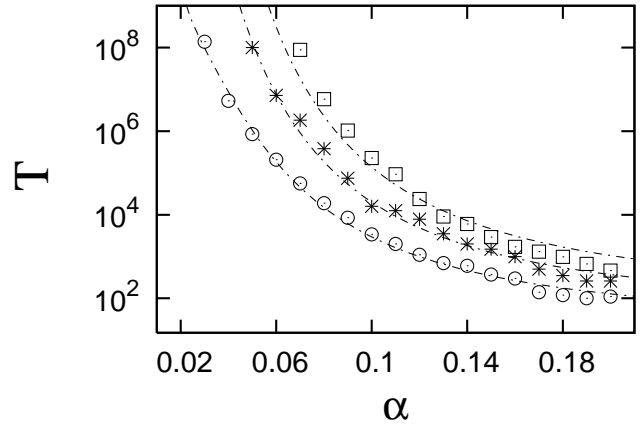


FIG. 2: Time measured in topplings per site until the inner block vanishes for $N = 64$ (circles), $N = 128$ (stars) and $N = 256$ (squares) as function of α ; the lines correspond to the function $T(\alpha, N) = \tilde{f}(\alpha)N^{\mu(\alpha)}$ as derived in the text.

in the later part of this calculation we will therefore replace $\tilde{\alpha}$ with α . When discussing the size distribution of avalanches further below, we will see that with increasing system size the proportion of avalanches larger than 1 decreases towards zero, implying that the average amount of energy passed to a neighbor approaches α even for larger values of α , and that most sites are exactly at the threshold when they topple, as was already observed numerically in [17, 32]. The assumption that the value of $\tilde{\alpha}$ is constant throughout time and throughout the system is a mean-field assumption. Due to the approximations involved, we can expect that our theory makes predictions that are qualitatively correct, but that the quantitative features could be different.

The balance equation reads

$$t_{ij} = g + \tilde{\alpha}(t_{i+1,j} + t_{i-1,j} + t_{i,j-1} + t_{i,j+1}). \quad (1)$$

Now, we have to take into account the structure of the system during the transient time. The outer part consists of patches of different sizes [24], and sites sitting in the same patch have to topple equally often for the patch to persist for a long time (which is observed by watching the system on the computer screen). The value of t_{ij} depends therefore on the distance to the boundary, which can be measured in terms of the number of patches, x , between site ij and the boundary. (We ignore here the fact that the system has corners, which should not fundamentally change the argument. In any case, one could consider a system that is periodic in one dimension and open in the other, in order to avoid corners altogether.) Sites in the disordered block topple like in a system with periodic boundary conditions, i.e. they receive the same input from all four neighbors. For these sites we have therefore $t = g + 4\alpha t$, or

$$t = t_0 \equiv \frac{g}{1 - 4\alpha}. \quad (2)$$

In terms of the parameter x , the above balance equation for the patchy part of the system becomes

$$t(x) = g + \tilde{\alpha}(t(x-1) + t(x+1) + 2t(x)), \quad (3)$$

or, in a continuum notation

$$\frac{1-4\tilde{\alpha}}{\tilde{\alpha}}t(x) - \frac{d^2}{dx^2}t(x) - \frac{g}{\tilde{\alpha}} = 0. \quad (4)$$

The boundary conditions are $t(0) = 0$ ($x = 0$ signifying the non-existent neighbor of a boundary site) and $t(d) = t_0$, with $d-1$ denoting the index of the patch next to the disordered block. The solution of the balance equation is then

$$t(x) = t_0 \left(1 - \frac{\sinh(\kappa(d-x))}{\sinh(\kappa d)} \right), \quad (5)$$

where κ is given by $\kappa = \sqrt{(1-4\alpha)/\alpha}$.

Next, we have to consider the advancement of the patchy structure into the inner part of the system. A site that is part of the inner block can become part of a patch only if the difference of its energy value z to that of its outer neighbor is less than α . This difference changes with time due to the different toppling rates. The patch next to the inner block topples less often than a neighbor of that patch, which is part of the inner block, the difference in the number of topplings per unit time being $t_0 [\sinh(\kappa)] / [\sinh(\kappa d)]$, which is obtained from (5) by inserting $x = d-1$. The difference in the number of topplings per unit time is identical to the rate of change of the difference in the energy value z between the two neighbors. When this difference has increased by 1, it has taken any intermediate value (in steps of size α) and has therefore certainly assumed a value smaller than α . At that moment, the site of the inner block becomes part of the patch. The time (or number of topplings per site) needed to add an additional site to a patch is therefore proportional to

$$n_c(\alpha, d) \sim \frac{\sinh \kappa d}{\sinh \kappa}. \quad (6)$$

In the limit of small α , $n_c(\alpha, d)$ is given by

$$n_c(\alpha, d) \sim \exp\left(\frac{d-1}{\sqrt{\alpha}}\right), \quad (7)$$

which has to be summed over all patches, weighted with the mean size of each generation of patches. The total transient time is therefore

$$T(\alpha, N) \sim \sum_{d=1}^{d_{max}(\alpha, N)} l(d)n_c(\alpha, d) \quad (8)$$

with $l(d)$ being the extension perpendicular to the boundary of a patch of type d . Below in Section IV, we will see that $l(d) \sim Q(\alpha)^{d-1}$, where Q is a function of α only

and approaches 1 (from above) for $\alpha \rightarrow 0$. From the condition

$$\frac{N}{2} = \sum_{d=1}^{d_{max}} l(d) \quad (9)$$

we obtain then

$$d_{max}(\alpha, N) \simeq \frac{\ln \left[\frac{N(Q-1)}{2q_0} + 1 \right]}{\ln Q} \simeq \frac{\ln \frac{N(Q-1)}{2q_0}}{\ln Q} \quad (10)$$

for large enough system sizes. q_0 is some constant (the extension of the patches of the first generation). The result for small α is therefore

$$T(\alpha, N) \simeq \left(\frac{N(Q-1)}{2q_0} \right)^{\mu(\alpha)} \exp\left(\frac{-2}{\sqrt{\alpha}}\right) \quad (11)$$

with the exponent $\mu(\alpha) = 1 + \frac{1}{\sqrt{\alpha \ln Q(\alpha)}}$. Using the ansatz $Q(\alpha) = \exp(f(\alpha))$, also motivated in Section IV, with a leading term $f(\alpha) \simeq A\alpha^a$ and A and a positiv, yields

$$\mu(\alpha) = 1 + \frac{1}{A\alpha^{a+0.5}} \quad (12)$$

and

$$T(\alpha, N) \simeq \left(\frac{N}{2q_0} f(\alpha) \right)^{\mu(\alpha)} \exp\left(\frac{-2}{\sqrt{\alpha}}\right) \quad (13)$$

Inspired by this result of the mean-field theory, we expect that the transient time is for small α given by an expression of the form

$$T(\alpha, N) \sim \tilde{f}(\alpha) N^{\mu(\alpha)}. \quad (14)$$

The data shown in Figure 2 agree with this expression. The numerical values of the parameter are $A \sim 32.6$ and $a \sim 1.262$. $\tilde{f}(\alpha)$ was fitted in the form $\tilde{f}(\alpha) \sim \exp[-V(\alpha + 0.01)^v + D]$, but any other expression could be equally valid. We would like to stress that this Ansatz was motivated by the mean field exponent μ for the leading dependence on N , which we think mirrors the true behavior correctly.

IV. CORRELATION FUNCTION AND CORRELATION LENGTH

As has become clear from the previous section, the size distribution of patches as function of N and α and of their distance from the boundary is an important feature of the system. It affects not only the transient time, but also the avalanche size distribution, which will be discussed in the next section.

We therefore investigate in this Section how the extension of the patches in the directions parallel and perpendicular to the boundary increases with the distance

from the boundary. For this purpose, we evaluate the correlation function

$$C(r) = \langle (z_{ij} - z_{i,j+r})^2 \rangle - \langle z_{ij} \rangle^2 \quad (15)$$

for a fixed distance i from the boundary for different times, starting again at a random initial configuration. We performed our simulations with systems that are periodic in the direction of the second coordinate, i.e. site $j + N$ is identical to site j . We chose $N = 2^{15}$ in order to obtain good statistics. The length of the system in the other direction was chosen just as large as needed, between 48 (for small α , where the invasion front proceeds very slowly) and 512 (for large α).

Figure 3 shows the correlation function for $\alpha = 0.08$ at distance 10 and distance 20 (measured in number of sites) from the boundary for three different times. One can see that at distance 10 the correlation function does not change any more with time, which means that the patch structure has been established at least up to this depth before the first measurement. We can furthermore conclude that the typical scale of the patches at a given distance from the boundary does not change any more when new patches are formed further inside. At dis-

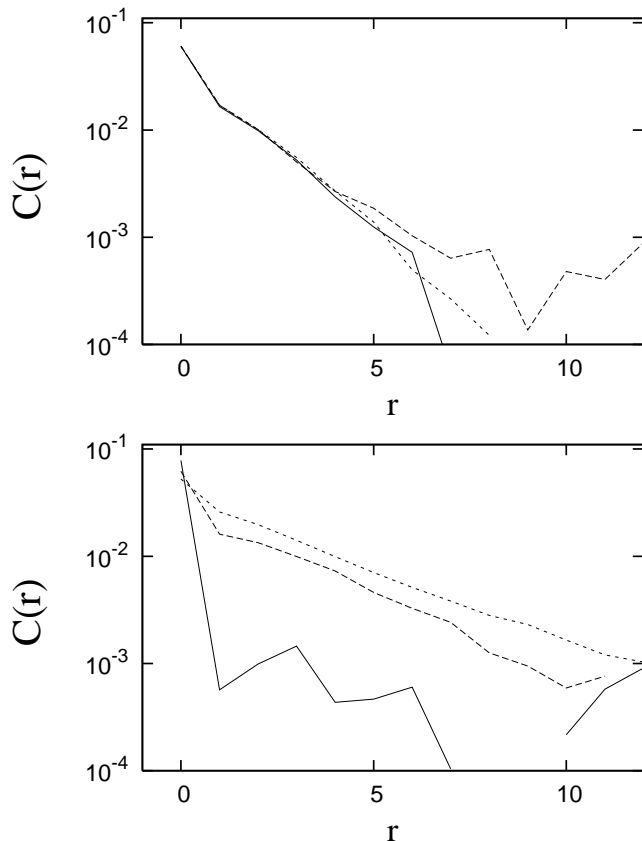


FIG. 3: Correlation function $C(r)$ for $\alpha = 0.08$ for a distance $d = 10$ sites (top) and $d = 20$ sites (bottom) from the boundary at three different times (after 2570 (solid line), 5130 (dashed line) and 12490 (dotted line) topplings per site).

tance 20, we see that the correlation function builds up

with time from zero to an exponentially decaying function $C(r) \sim e^{-r/\xi}$. Figure 4 shows the correlation length ξ for $\alpha = 0.12$ as function of the distance to the boundary for three different times. In the region where the patches are already present, ξ increases as a power law in the distance from the boundary, and then falls down to zero. We see again that ξ remains constant once the patches have emerged. The large fluctuations seen before the decrease to zero occur in the region where the patches are just being formed. Due to large fluctuations in space, the averaging over the length of the system does not lead to a smooth curve for the system sizes used.

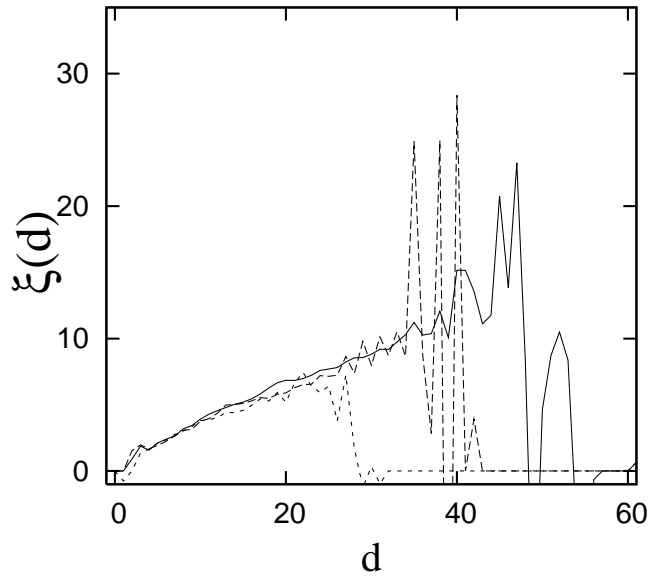


FIG. 4: Correlation length ξ as function of the distance d to the boundary for $\alpha = 0.12$ after 650, 1290 and 2570 topplings per site.

Figure 5 shows the correlation length as function of depth for different values of α . The data are in good agreement with a linear increase of ξ with the distance d from the boundary, but with a factor that decreases with decreasing α . However, we cannot rule out a power law $\xi \sim d^\eta$ with an exponent $\eta < 1$ that increases with α .

The linear (or power-law) increase of the correlation length together with the patchy structure leads to the following schematic picture (see Fig. 6):

The characteristic size of patches increases with distance from the boundary. From one generation of patches to the next, the width and height of the patches increase with factors $P(\alpha)$ and $Q(\alpha)$ respectively. In the case $\eta = 1$, we have $P = Q$. (Of course, the patches at a given distance from the boundary do not all have exactly the same size, but a size of the indicated order of magnitude.) From snapshots of the systems, it is clear that $P(\alpha)$ and $Q(\alpha)$ increase with α . Furthermore, there must be a lower bound of 1 to both factors in the limit $\alpha \rightarrow 0$. Thus, we can write $Q(\alpha) = \exp(f(\alpha))$ with a monotonically increasing function $f(\alpha)$ and $f(0) = 0$. The leading

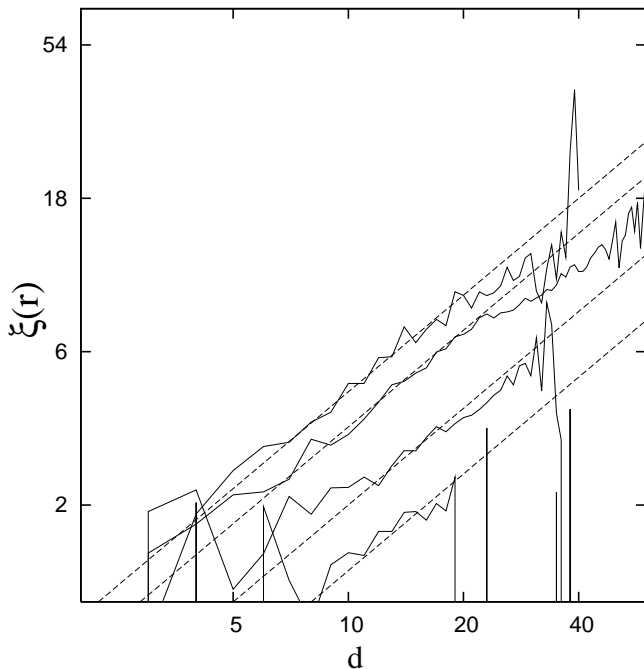


FIG. 5: Correlation length ξ as function of the distance to the boundary for $\alpha = 0.06, 0.09, 0.12$ and 0.15 (from bottom to top) at the largest times simulated for a given value of α (solid lines); The dashed lines correspond to lines of slope 1

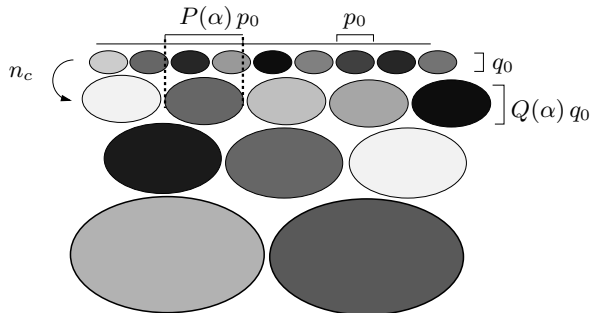


FIG. 6: Schematic view of the system's structure: the width and height of patches increase with a power law in the distance to the boundary. Different generations of patches are coupled via n_c , the increase in the size of the patches is $P(\alpha)$ parallel to the boundary and $Q(\alpha)$ perpendicular to it, starting with a size $s_0 = p_0 q_0$.

dependence on α can be expected to be $f(\alpha) = A\alpha^a$ with positive A and a .

The correlation length in the i th generation of patches (counting from the boundary) is

$$\xi \sim P^i \sim d^\eta \quad (16)$$

and the distance from the boundary is

$$d \sim \sum_{j=1}^i Q^j. \quad (17)$$

Based on this picture, we can write down an expression for the size distribution of patches, which will be an important tool when discussing the size distribution of avalanches. A line at the distance d from the boundary cuts through $\sim N/\xi h$ new patches of width ξ and height $h \sim \xi^{1/\eta}$ through which the neighboring line does not cut, since there are $\sim N$ sites along this line. The width distribution of patches is therefore given by

$$n_P(\xi)d\xi = \frac{N}{\xi h} d(d),$$

leading to

$$n_P(\xi) \sim \frac{N}{\xi^2}, \quad (18)$$

Transforming this into the size distribution $n_P(s)$ with $s \sim \xi h$, we obtain

$$n_P(s) \sim N s^{-\frac{1+2\eta}{1+\eta}}. \quad (19)$$

In the likely case that $\eta = 1$, we have an exponent $-3/2$ in the size distribution of patches. Expressed in terms of P and Q instead of η , the last equation becomes

$$n_P(s) \sim N s^{-\frac{\ln P}{\ln PQ} - 1}, \quad (20)$$

where P and Q depend on α . This expression can also be obtained directly from the recursion relation

$$\int n_P(sP(\alpha)Q(\alpha)) ds = \int n_P(s) \frac{1}{P(\alpha)} ds, \quad (21)$$

where the integral is taken over one generation of patch sizes.

V. AVALANCHE SIZE DISTRIBUTION

Now we turn to the size distribution of avalanches in the stationary state. We made sure that the process of patch formation has reached the center of the system, before we evaluated the avalanche size distribution.

In view of the results in Section III, we are now in the position to check how trustworthy the results reported in the literature are. As was already pointed out by Grassberger [12], transient times are extremely long, and the first publications [1, 33, 34, 35] can have considered stationary systems only for the largest values of α .

It appears that many avalanche size distributions presented in the last decade were actually obtained during the transient stage. We can check this only when the authors state how many initial avalanches they discarded for given N and α . Unfortunately, not all authors write how they decided if the system is in the stationary state. By observing statistical properties and comparing them at different times, one can be misled to believe that the system has become stationary, although the advancement of the patches has only become very slow. Generally, the

larger α and the smaller the system size, the more likely is it that the published avalanche size distributions were obtained in the stationary state. For example, the results published in [16, 23] with $L = 25, 45$ were probably not taken in the stationary state for α below 0.2. Even Grassberger was evaluating avalanche size distributions during the transient stage in some parameter regimes.

While taking small system sizes has the advantage of reaching the stationary state fast, they have the disadvantage of being strongly affected by finite-size effects. It is therefore very difficult to predict the avalanche-size distributions in the thermodynamic limit.

Figure 7 shows avalanche size distributions for varying α with fixed N and for varying N with fixed α . The value of N in the top figure has been chosen small enough that the system could reach the stationary state even for the smallest value of α , which was 0.03. We can discern the following features:

1. At least for value of α smaller than 0.17, the avalanche size distribution is no power law. A fit of the form $n(s) \sim s^{-\tau(\alpha)-\sigma(\alpha)\ln s}$ approximates the data much better than a pure power law.
2. $n(s)$ changes its shape with increasing N , implying that the system size affects the relative weight even of small avalanches, at least for the system sizes considered. This effect is stronger for smaller α . Only for the largest value of α is the main effect of the finite system size a rather sharp cutoff at N^2 .
3. The weight of avalanches of size 1 increases with increasing system size, while the weight of all larger avalanches decreases as $1/N$ (see below).

In the following, we will explain these features based on the results obtained in the previous sections, and on what is known from literature. Described in words, the scenario is the following: Patches persist for a long time before they change their shape [24], due to an avalanche that enters the patch from outside [12], and patches further inside the system are rearranged less often. Large, patch-wide avalanches are mainly triggered at the boundaries of the system. Whenever a patch-wide avalanche took place, there is a sequence of ‘aftershocks’ with decreasing size according to Omori’s law [18], and after a short time there occur mostly single topplings within a patch, until the next large avalanche comes from a patch of the previous generation.

Let us quantify these statements. Analogous to the process of synchronizing neighboring sites discussed in Section III, neighboring patches also need a certain number $n_c(\alpha)$ of patch-wide avalanches in the patch closer to the boundary, before the inner patch experiences a patch-wide avalanche. This can be evaluated using Eq. (5) for the situation that $d = d_{max}$. We therefore obtain the recursion relation (compare (21))

$$\int n_{pw}(P(\alpha)Q(\alpha)s) ds = \int n_{pw}(s) \frac{1}{P(\alpha)n_c(\alpha)} ds, \quad (22)$$

for the size distribution of patch-wide avalanches. If n_c was independent of the generation number i , this would result in a power law $n_{pw}(s) \propto Ns^{-\tau(\alpha)-1}$ with an exponent

$$\tau(\alpha) = \frac{\ln P(\alpha)n_c(\alpha)}{\ln P(\alpha)Q(\alpha)}. \quad (23)$$

For systems not too big, and for large enough α , there are only a few generations, and the approximation of a constant n_c is not too bad. Evaluating Eq. (5) for small α , we obtain the following result for n_c that depends on the generation index i ,

$$n_c(\alpha, i) \sim \exp\left(\frac{i-1}{\sqrt{\alpha}}\right), \quad (24)$$

(see also equation (7)). Iterating Equation (22), we need to evaluate the product

$$\prod_{j=1}^i \left(\frac{1}{P(\alpha)n_c(\alpha, j)} \right) = \left(\frac{1}{P(\alpha)} \right)^i \exp\left(-\frac{i(i-1)}{2\sqrt{\alpha}}\right), \quad (25)$$

which leads (using $\ln i \sim \ln s / \ln PQ$) to size distribution of patch-wide avalanches of the form

$$n_{pw}(s) \sim Ns^{-\tau(\alpha)-1-\sigma(\alpha)\ln s}, \quad (26)$$

where $\tau(\alpha)$ and $\sigma(\alpha)$ are given by

$$\begin{aligned} \tau(\alpha) &= \frac{1}{\ln(P(\alpha)Q(\alpha))} \left(\ln P(\alpha) - \frac{1}{2\sqrt{\alpha}} \right) \\ \sigma(\alpha) &= \frac{1}{2\sqrt{\alpha}(\ln(P(\alpha)Q(\alpha)))^2} \end{aligned} \quad (27)$$

Now, we have to estimate the effect of ‘aftershocks’ on the size distribution of avalanches. These aftershocks will lead to an avalanche-size distribution that differs from that of the patch-wide avalanches. Aftershocks are avalanches that occur within a patch after a patch-wide avalanche. We assume that their size distribution is a power law with a cutoff at the size of the patch. This is motivated by the finding that systems that are dominated by one large patch display a power-law size distribution of avalanches (see also [18, 19]). Therefore, we set

$$n_{as}(s|s') = s'^{\tau_0} s^{-\tau_0} \theta(s' - s),$$

with $n_{as}(s|s')$ being the number of aftershock avalanches of size s in a patch of size s' , and with an exponent τ_0 , which has a value around 1.8 (i.e., the value found in [7] for systems that have essentially one large patch). The size distribution of avalanches is then given by

$$\begin{aligned} n(s) &\propto N \int_s^\infty n_{pw}(s') n_{as}(s|s') ds' \\ &= Ns^{-\tau_0} \int_s^\infty s'^{-\tau(\alpha)-1-\sigma(\alpha)\ln s'} s'^{\tau_0} ds' \\ &\sim Ns^{-\tau(\alpha)-\sigma(\alpha)\ln s} \end{aligned} \quad (28)$$

apart from a factor containing terms that depend on $\ln s$. Thus, the avalanche-size distribution is not a power law, but it has an exponent that depends logarithmically on s . As we have shown above, the data agree well with such a law. Figure 8 shows our results obtained for the coefficients σ and τ by fitting the avalanche-size distribution with the expression (28). Although we can expect that the data are affected by finite-size effects particularly for small α , we see that the functions $\sigma(\alpha)$ and $\tau(\alpha)$ show a behavior that is in agreement with our expressions (27): For small α , τ decreases rapidly and will eventually become negative, while σ tends to large positive values.

The cutoff of the avalanche-size distribution is determined by the size of the largest patch. As this size becomes smaller with smaller α , the cutoff decreases also. Furthermore, since larger patches make a contribution to smaller avalanches via aftershocks, the effect of the finite system size will be felt down to avalanche sizes much smaller than the largest patch. This is what is observed in the data.

Finally, let us discuss the weight of avalanches of size 1. After a patch-wide avalanche and the resulting aftershocks, a patch has single topplings (i.e., avalanches of size 1), just as a system with periodic boundary conditions, until a new patch-wide avalanche comes from outside. The total number of avalanches of size larger than 1 per unit time is given by

$$\int_2^{\infty} n(s) ds \propto N.$$

However, the total number of topplings per unit time is proportional to the number of sites in the system N^2 . We conclude, that only a proportion of the order $1/N$ of avalanches has a size larger than 1.

VI. CONCLUSION

In this paper, we have shown that the transient time for the OFC model increases as function of the system size N and the coupling parameter α as $T(\alpha, N) \sim N^{\alpha^{-\mu}}$, apart from corrections depending on α which do not affect this leading non-analytical behavior. This finding is in contrast to earlier predictions that the transient time increases as a power law with system size, or that the transient time becomes infinite when α is smaller than some value. We obtained these results by performing a mean-field like calculation for the number of topplings per site and for the advancement of the patchy structure into the inner part of the system.

Furthermore, by evaluating the correlation length of the energy values we found that the size of the patches increases as a power law with the distance from the boundary, leading to power law size distribution of the patches. Even if we assume that the size distribution of avalanches

within a patch is a power law, we find based on the results mentioned so far that the overall size distribution of avalanches is no power law, but has a logarithmic dependence in the exponent on the avalanche size, i.e., is of a log-Poisson form. This finding is supported by the simulation data and is valid at least for smaller α , where the system is not dominated by one large patch.

We obtained our simulation results by using an efficient algorithm, however, the sharp increase of the transient time with system size especially for small α made it impossible to study system sizes as large as necessary to see the true asymptotic behavior of the avalanche size distributions.

Our findings are interesting for several reasons. First, the OFC model appears to show many features found in real earthquakes. As far as earthquake predictability [36] or Omori's law [18, 19] are concerned, this model appears to be closer to reality than others. If α is chosen above 0.17, the avalanche size distribution agrees best with the Gutenberg-Richter law [7]. Second, the OFC model demonstrates that apparent power laws need not reflect a true scale invariance of the system. We expect that this is true for many natural driven systems. Due to the dynamics of the model, there occur avalanches of all sizes, however the mechanisms producing these avalanches are different on different scales. Large avalanches are mainly patch-wide avalanches, while smaller avalanches occur within patches during a series of foreshocks or aftershocks. Also, avalanches at different distance from the boundaries have different sizes. The observed "power laws" are thus *dirty* power laws, which appear like power laws over a wide range of parameters and over a few decades on the avalanche size axis, while the "true" analytical form is no power law. Third, the lack of a true scale invariance is accompanied by a decreasing weight of avalanches larger than 1 with increasing system size. This indicates again that the avalanche size distribution of the model does not approach some asymptotic shape with increasing system size, but that the weights of different types of avalanches shift with the system size. This effect has most clearly been seen in one dimension, where the distributions split into a α dependent part at small avalanche sizes and a peak at sizes of order of the system size. Fourth, the extremely long transient times point to the possibility the some driven natural systems with avalanche-like dynamics are not in the stationary regime either.

Acknowledgments

This work was supported by the Deutsche Forschungsgemeinschaft (DFG) under Contract No Dr300/3-1 and Dr300/3-2.

-
- [1] Z. Olami, H. J. S. Feder, and K. Christensen, *Phys. Rev. Lett.* **68**, 1244 (1992).
- [2] S. Manna, L. Kiss, and J. Kertész, *J. Stat. Phys.* **61**, 923 (1990).
- [3] P. Bak, C. Tang, and K. Wiesenfeld, *Phys. Rev. Lett.* **59**, 381 (1987).
- [4] T. Hwa and M. Kardar, *Phys. Rev. Lett.* **62**, 1813 (1989).
- [5] G. Grinstein, D. H. Lee, and S. Sachdev, *Phys. Rev. Lett.* **64**, 1927 (1990).
- [6] S. Lise and M. Paczuski, *Phys. Rev. E* **64**, 046111 (2001).
- [7] S. Lise and M. Paczuski, *Phys. Rev. E* **63**, 036111 (2001).
- [8] G. Miller and C. Boulter, *Phys. Rev. E* **68**, 056108 (2003).
- [9] J. de Carvalho and C. Prado, *Phys. Rev. Lett.* **84**, 4006 (2000).
- [10] G. Miller and C. Boulter, *Phys. Rev. E* **66**, 016123 (2002).
- [11] A. Middleton and C. Tang, *Phys. Rev. Lett.* **74**, 742 (1995).
- [12] P. Grassberger, *Phys. Rev. E* **49**, 2436 (1994).
- [13] C. Pérez, A. Corral, A. Díaz-Guilera, K. Christensen, and A. Arenas, *Int. J. Mod. Phys. B* **10**, 1111 (1996).
- [14] N. Mousseau, *Phys. Rev. Lett.* **77**, 968 (1996).
- [15] I. Jánosi and J. Kertész, *Physica A* **200**, 179 (1993).
- [16] H. Ceva, *Phys. Rev. E* **52**, 154 (1995).
- [17] B. Drossel, *Phys. Rev. Lett.* **89**, 238701 (2002).
- [18] S. Hergarten and H. Neugebauer, *Phys. Rev. Lett.* **88**, 238501 (2002).
- [19] S. H. A. Helmstetter and D. Sornette, *Phys. Rev. E* **70**, 046120 (2004).
- [20] O. Ramos, E. Altshuler, and K. Måløy, *Phys. Rev. Lett.* **96**, 098501 (2006).
- [21] B. Drossel and F. Wissel, *New Journal of Physics* **7**, 5 (2005).
- [22] S. Lise, *J. Phys. A* **35**, 4641 (2002).
- [23] H. Ceva, *Phys. Lett. A* **245**, 413 (1998).
- [24] S. Bottani and B. Delamotte, *Physica D* **103**, 430 (1997).
- [25] K. Christensen, D. Hamon, H. Jensen, and S. Lise, *Phys. Rev. Lett.* **87**, 039801 (2001).
- [26] J. de Carvalho and C. Prado, *Phys. Rev. Lett.* **87**, 039802 (2001).
- [27] S. Lise and H. Jensen, *Phys. Rev. Lett.* **76**, 2326 (1996).
- [28] M. Chabanol and V. Hakim, *Phys. Rev. E* **56**, R2343 (1997).
- [29] H. Broecker and P. Grassberger, *Phys. Rev. E* **56**, 3944 (1997).
- [30] S. Pinho, C. Prado, and O. Kinouchi, *Physica A* **257**, 488 (1998).
- [31] R. Burridge and L. Knopoff, *Bull. Seismol. Soc. Am.* **57**, 341 (1967).
- [32] G. Miller and C. Boulter, *Phys. Rev. E* **67**, 046114 (2004).
- [33] K. Christensen, Z. Olami, and P. Bak, *Phys. Rev. Lett.* **68**, 2417 (1992).
- [34] Z. Olami and K. Christensen, *Phys. Rev. A* **46**, R1720 (1992).
- [35] K. Christensen and Z. Olami, *Phys. Rev. A* **46**, 1829 (1992).
- [36] S. Pepke and J. Carlson, *Phys. Rev. E* **40**, 234 (1994).

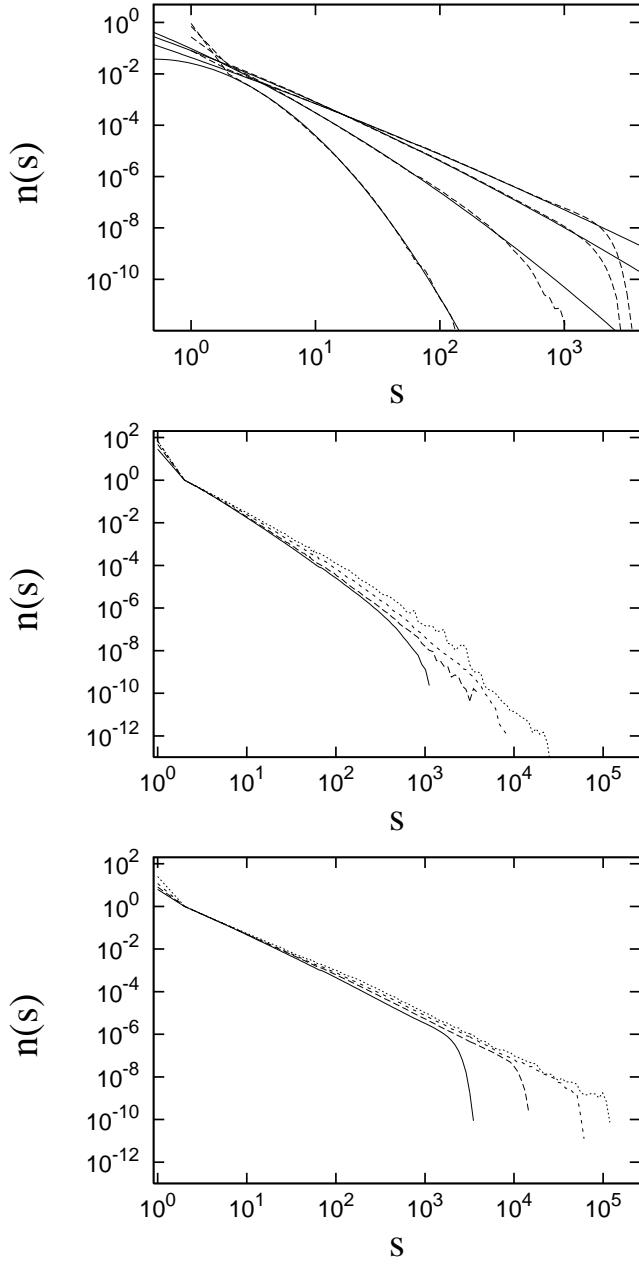


FIG. 7: Size distribution of avalanches for different parameter; top: system size $N = 64$ and $\alpha = 0.03, 0.08, 0.13, 0.18$, steeper curves correspond to smaller α ; the s -axis extends up to the total number of sites 4096; the distributions are normed on the total number of topplings; solid lines correspond to $f(s) \sim s^{-\tau - \sigma \ln s}$. middle and bottom: size distribution for system sizes $N = 64, 128, 256, 512$; $\alpha = 0.09$ (middle) and $\alpha = 0.17$ (bottom); the distributions are divided by $n(2)$.

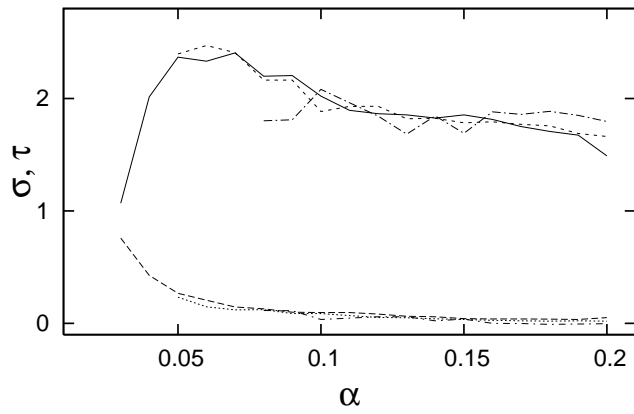


FIG. 8: The coefficients $\sigma(\alpha)$ (lower set of curves) and $\tau(\alpha)$ (upper set) as function of α as found by fitting the distributions $n(s)$ for $N = 64, 128$ and 256 for those values of α where stationary systems were reached.